SpezialForschungsBereich F 32

Karl–Franzens Universität Graz
Technische Universität Graz
Medizinische Universität Graz

Feasibility of lung imaging using magnetic induction tomography

Doğa Gürsoy Hermann Scharfetter

SFB-Report No. 2009–013 April 2009

A–8010 GRAZ, HEINRICHSTRASSE 36, AUSTRIA

Supported by the
Austrian Science Fund (FWF)

Der Wissenschaftsfonds.

SFB sponsors:

- **Austrian Science Fund** (FWF)
- **University of Graz**
- **Graz University of Technology**
- **Medical University of Graz**
- **Government of Styria**
- **City of Graz**

Feasibility of lung imaging using magnetic induction tomography*

Doğa Gürsoy and Hermann Scharfetter †

April 13, 2009

Abstract

Magnetic induction tomography (MIT) is a low resolution imaging modality and attempts to reconstruct the interior conductivity distribution of the body. In MIT, the transmitter coils induce eddy currents in the body and the response field caused by the conductivity perturbations is sensed by an array of receiver coils. All the applications that were offered for electrical impedance tomography (EIT) are also a potential application for MIT. However, unlike EIT, MIT can look better through insulating tissues, e.g. ribcage which is made of bone tissue, and since the method is contactless, it does not suffer from the poor electrode contact. In this paper, the feasibility of lung imaging was investigated using a realistic thorax model of which the tissue boundaries were segmented from MRI images. The images were reconstructed from different simulated datasets, i.e. static, temporal and spectral datasets, to cover all the potential imaging approaches that MIT can offer. It was shown that the lung imaging is a feasible application for MIT, however, still some software and hard-ware improvements are essential before a clinical usage.

Keywords: Magnetic induction tomography, lung imaging, bio-impedance measurements, image reconstruction, finite element method.

1 Introduction

The ultimate goal of medical MIT is to image the electri-cal conductivity within the region of interest. The static, temporal and spectral conductivity differences between the tissues permit imaging of several physiological processes and physiological disorders using MIT. The methodology is as follows: The tissues are excited via magnetic induction using an array of transmitting coils which are positioned around the region of interest so that an eddy current density is induced

*This work was supported by the Austrian Science Fund under the SFB Project F32-N18 and submitted to Medical Physics and Biomedical Engineering World Congress 2009.

†D. Gürsoy and H. Scharfetter are with the Institute of Medical Engineering, Graz University of Technology, Austria. e-mail: guersoy@tugraz.at

in the desired region. Then, the magnetic field perturbations due to the changes in the eddy current field are sensed by receiver coils. The operating frequency range for a typical MIT system is from several tens of kHz up to several tens of MHz and covers the β-dispersion region of many biological tissues of interest. Several systems have been built and most of them consist of 16 transmitter and 16 receiver channels encircling the body (For a comprehensive review see, e.g. [1]).

Although lung imaging with EIT has been extensively investigated [2], there has not yet been a profound investi-gation for MIT. Unlike EIT, MIT can look better through insulating tissues, e.g. ribcage which is made of bone tissue, and since the method is contactless, it does not suffer from the poor electrode contact. In this paper, the feasibility of lung imaging was investigated by simulations using a realis-tic thorax model. The thorax model was constructed using the tissue boundaries segmented from MRI images and consisted of four different tissue types: muscle, lung, heart and liver. The conductivity spectrum for each different tissue was assigned based on a parameterized Cole equation [3]. Within each tissue the conductivity was assumed ho-mogenous and isotropic.

2 Methods

2.1 Forward problem

The forward problem of MIT requires the solution of a nonlinear eddy current problem to find the induced electric field in the body due to the primary coil excitation. The governing partial differential equations for the solution of the electric scalar potential ϕ, is as follows,

$$\nabla \cdot \kappa \nabla \phi = -jw\mathbf{A} \cdot \nabla \kappa \quad (1)$$

$$\nabla \phi \cdot \mathbf{n} = -jw\mathbf{A} \cdot \mathbf{n} \quad (2)$$

where $\kappa = \sigma + jw\epsilon$ is the admittivity of the body, w is the operating frequency of the excitation field and $\mathbf{n}$ is the normal vector directed outward from the body surface. The right hand side of the equation is the source term and $\mathbf{A}$ is the magnetic vector potential in free space which was precomputed analytically.

The equation set was discretisized by finite element method assuming constant admittivity in each voxel (see, e.g. [4]). Thus, the source term of (1) vanishes. Once ϕ was computed, the induced electric field was found from,

$$\mathbf{E} = -\nabla \phi - jw\mathbf{A}. \quad (3)$$

To compute the voltages in the receiver coils, according to the reciprocity theorem, it suffices to compute the adjoint electric field $\mathbf{E}_a$ assuming a unity excitation in the receiver coil as if it was a transmitter,

$$v = \int_{\Omega} (\kappa \mathbf{E}_d) \cdot \mathbf{E}_a d\Omega \quad (4)$$

where Ω is the body volume and $\mathbf{E}_d$ as the electric field generated in the body by the transmitters. By using (4), one can generate a maximum number of $m \times n$ complex independent data assuming n transmitters and m receivers. Although the voltage signal is complex, the imaginary component (in phase component of the voltage with the excitation current) suffers from noise due to some hardware limitations [5]. Therefore, this paper will only use the real part of the signal which is dependent on the conductivity distribution.

2.2 Inverse problem

The inverse problem of MIT is defined as estimating the conductivity distribution in the body from the voltage data. The inversion is severely ill-posed due to inaccurate data. Therefore, the solution needs regularization and an accurate forward model. The image reconstruction of MIT have commonly been realized by assuming a linear relationship between the data and the conductivity changes,

$$\frac{\partial v}{\partial \sigma} = \mathbf{S}\Delta\sigma = \Delta v \tag{5}$$

defining $\mathbf{S}$ as the Jacobian or so called the sensitivity matrix. The sensitivity of the p^{th} data to the conductivity perturbation of the q^{th} voxel was computed from,

$$\mathbf{S}_{pq} = \left(\mathbf{E}_{d,q} \cdot \mathbf{E}_{a,q}\right) \Delta\Omega \tag{6}$$

where $\mathbf{E}_d$ and $\mathbf{E}_a$ are the direct and adjoint electric fields for a specific transmit-receive coil pair and $\Delta\Omega$ denotes the volume of the corresponding voxel. The least square approximation, usually with an additional L_2-norm penalty term (for stability), was adopted for image reconstruction [6] and is expressed as follows,

$$\Delta\sigma = (\mathbf{S}^T\mathbf{S} + \lambda\mathbf{R})^{-1}\mathbf{S}^T\Delta v \tag{7}$$

where $\mathbf{S}^T\mathbf{S}$ is an approximation of the Hessian of the forward operator for a particular σ, $\mathbf{R}$ is the regularization matrix and λ is the regularization parameter. In this study $\mathbf{R}$ was chosen as the identity matrix.

Reconstruction of static, temporal and spectral conductivity images is possible by different excitation and recording schemes. To obtain the difference dataset, in principle, the empirical dataset obtained, let's say at a specific frequency, is subtracted from a reference dataset. When the reference dataset was simulated from a specific (usually uniform) model, it is called static (or state differential) imaging. Similarly the reference dataset can be acquired at a different operating frequency or at different times, which lead to temporal (or time differential) imaging and spectral (or frequency differential) imaging, respectively.

2.3 Model

The model for the simulation was obtained by segmenting the thorax MRI images to construct a three dimensional volume (see, Figure 1). MIT is a low

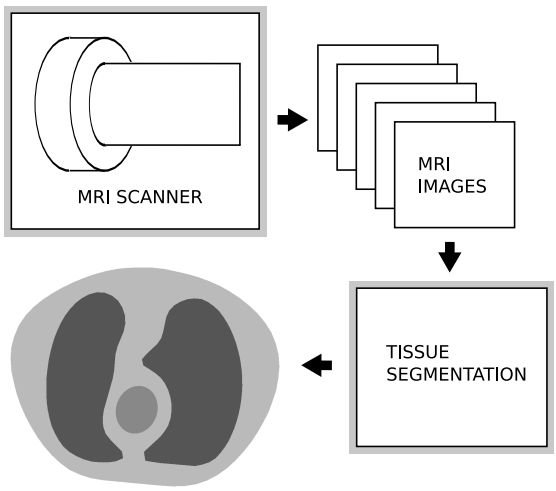

Figure 1: The demonstration of the modeling process. The thorax model was constructed using the tissue boundaries segmented from MRI images.

Table 1: The conductivity values of different tissues excited at 100 kHz and 600 kHz. The values were computed based of the parametrized Cole-cole equation. All units are S/m.

Tissue (σ)	100 kHz	600 kHz
Lung	0.1074	0.1258
Heart	0.2151	0.2918
Muscle	0.3618	0.4613
Liver	0.0846	0.1581

resolution modality and imaging of small details seems infeasible, therefore, the model was constructed roughly by considering only the extended tissue groups. The major tissues: muscle, lung, heart and liver were used in the model. The conductivity spectrum for each different tissue was assigned based on a parameterized Cole equation and the resulting conductivity values were listed in Table 1 for different two operating frequencies. The discretization of the volume was established by the advancing front method using a commercial software (Hypermesh, copyrighted by Altair Inc.) and consists of approximately 100 000 elements.

The transmitter and the receiver arrangement are depicted in Figure 2. 16 transmitter coils of 30 mm radius encircle the thorax in two rings positioned radial in a zigzag arrangement and 16 receivers of 30 mm radius were positioned in front of the transmitters.

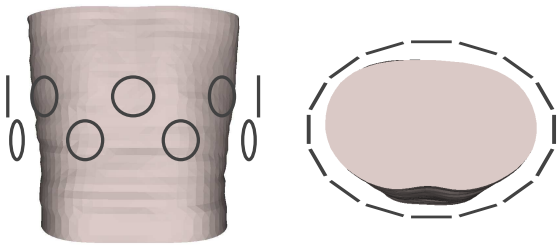

Figure 2: The simulation arrangement. 32 transmitter coils of 30 mm radius encircle the thorax in two rings positioned radially in a zigzag arrangement and 32 receivers of 30 mm radius were positioned in front of each transmitter.

3 Results

Static image of the central slice at 600 kHz is given in Figure 3. Using the empty space measurements for the reference dataset usually engender to poor images, therefore, the reference dataset were simulated by using a uniform conducting thorax to which the conductivity of the muscle tissue at 600 kHz was assigned. In the reconstructed image, it was possible to distinguish both lungs and the right lung was noted to be larger in magnitude, as expected.

Spectral (frequency differential) image of the central slice is given in Figure 4. The reference and the measurement datasets were obtained at 100 kHz and 600 kHz, respectively, and were used to form the difference dataset. From the image, it is still possible to differentiate the lungs; and, the image showed similar characteristics as the static image. The right lung conductivity estimates was larger than the left lung.

The temporal (time differential) image of the central slice at 600 kHz is depicted in Figure 5. The conductivity of inflated and deflated lungs was chosen to simulate the peaks of the respiration cycle. From the image, it is still possible to differentiate the lungs; however, the static and spectral images showed better distinguishability. The inversion tends to reconstruct both lungs as a whole; therefore, considering noise and increased regularization it may not be possible to distinguish each lung separately.

The heart was not identified in any of the images. The reason is possibly that the sensitivity is very poor in the center regions and the conductivity changes in surfacenear regions cloaked the heart reconstruction. Similarly liver was not showed up in any of the reconstructions, possibly, due to its far location according to the excitation and the sensors.

In all images, the artifacts close to the thorax surface appeared near the proximity of the sensor positions which were noted in most reconstructions regardless whether EIT or MIT was used. They are present in the images of both modalities due to similar characteristics of the singular vectors corresponding to the largest singular values of the sensitivity matrix.

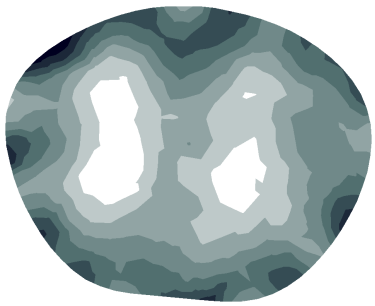

Figure 3: Static image of the central slice. The excitation frequency was 600 kHz. The reference dataset were simulated by assigning the conductivity of the muscle tissue to the background in order to form a difference dataset.

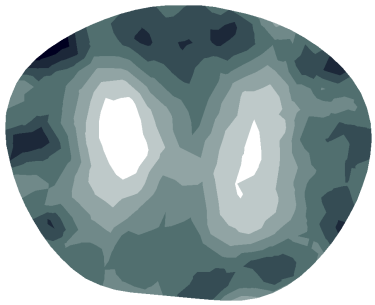

Figure 4: Spectral (frequency differential) image of the central slice. The dataset simulated at 100 kHz and 600 kHz were used to form the difference dataset.

4 Discussions and Conclusions

The linearity assumption for the solution of the inverse problem may lead to undesired conductivity estimates when the change of the conductivity distribution is too high. This seems an important issue especially for thorax imaging where the lung tissue is distributed extensively and the changes hardly fulfill the linearity assumption. Applying more iteration may not always solve this problem, since the iterative algorithm usually converges to a local solution. Therefore, better *prior* information should be provided to ensure feasible solutions.

In this work, the simulations were realized assuming a motionless model. Considering a realistic setting, the body or the internal organs can move during data acquisition due to respiration, heart beats, etc. and leads to artifacts [7]. In spectral imaging, the difference datasets are acquired simultaneously which automatically cancels the motion artifacts arose in the images. However, static and temporal images usually suffer from the movement of the patient during data acquisition.

The conductivity of the tissues varies with gender, age and condition of the patients, which makes it essential to determine the corresponding statistics to

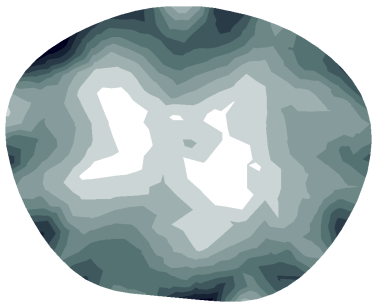

Figure 5: Temporal (time difference) image of the central slice. The excitation frequency was 600 kHz. To simulate temporal dependence, the data simulated from deflated and inflated lung models were used to form the time difference dataset.

the model and to include this information as a prior assumption. In this work, a deterministic thorax model was used to explore the basic aspects of lung imaging and to provide a computational toolbox for the analysis. The next step would be to investigate the outcomes of a stochastic thorax model incorporating the conductivity uncertainties of the tissues.

As a conclusion, the feasibility of lung imaging using MIT was explored. A realistic thorax model was constructed using MRI images and used for the analysis. The images were reconstructed by different datasets, i.e. static, temporal and spectral to cover all the potential imaging approaches that MIT can handle. It was shown that the lung imaging is a potential application for MIT, however, there are still some software and hardware improvements needed for a clinical usage.

Acknowledgements

We thank Patricia Brunner for her aid concerning the mesh generation issues.

References

[1] H. Griffiths, Magnetic Induction Tomography, *Meas. Sci. Technol.*, vol. 26, pp. 1126-31, 2001.

[2] D. Holder, *Electrical Impedance Tomography: Methods, History and Applications*, Inst of Physics Pub Inc, 2005.

[3] S. Gabriel, R. W. Lau, C. Gabriel, The dielectric properties of biological tissues: III. Parametric models for the dielectric spectrum of tissues, *Phys Med Biol*, vol. 41, pp. 2271-93, 1996.

[4] N. G. Gençer and M. N. Tek, Forward problem solution for electrical conductivity imaging via contactless measurements, *Phys. Med. Biol.*, vol. 44, pp. 927-40, 1999.

[5] H. Scharfetter, R. Casanas, J. Rosell, Biological Tissue Characterization by Magnetic Induction Spectroscopy (MIS): Requirements and Limitations, *IEEE Tran. Bmed. Eng.*, vol. 50, pp. 870-80, 2003.

[6] R. Merwa, K. Hollaus, B. Brandstatter, H. Scharfetter, Numerical solution of the general 3D eddy current problem for magnetic induction tomography (spectroscopy), *Physiol. Meas.*, vol. 24, pp. 545-54, 2003.

[7] D. Gürsoy and H. Scharfetter, Reconstruction artefacts in magnetic induction tomography due to patient's movement during data acquisition *Physiol. Meas.*, in press, 2009.